THE ULTRASTRUCTURE OF THE NEXUS

A Correlated Thin-Section and Freeze-Cleave Study

N. SCOTT McNUTT and RONALD S. WEINSTEIN

From the Departments of Pathology, Harvard Medical School and the Massachusetts General Hospital; and the Mixter Laboratory for Electron Microscopy, Neurosurgical Service, Massachusetts General Hospital, Boston, Massachusetts 02114

ABSTRACT

A correlation is made between the appearances of the nexus ("gap junction") as revealed by thin-section and by freeze-cleave electron microscopy techniques. These methods reveal different aspects of a complex subunit assembly forming the nexus membranes. In thin sections, the nexus is formed by the very close apposition of two "unit" membranes. The electron-opaque tracer, colloidal lanthanum hydroxide, outlines an aspect of electron-lucent subunits that project into the central region of the nexus. The freeze-cleave technique demonstrates novel membrane faces that are generated from within the interior of plasma membranes by splitting them into two lamellae (Lm): Lm 1 adjacent to the cytoplasm, and Lm 2 adjacent to the extracellular space. Each of the two membranes forming the nexus can be split into these two lamellae. On the new face of Lm 1, particles approximately 50 A in diameter are closely packed in an array which is often hexagonal with a 90–100 A center-to-center spacing. The two apposed lamellae (Lm 2-Lm 2) of the nexus are constructed of sheets of subunits in a similar array. The Lm 1 particles appear to extend into the Lm 2 subunits to form macromolecular complexes. The Lm 2 subunits extend to the center of the nexus to form the contacts outlined by lanthanum in sections. It is postulated that central hydrophilic channels may extend through the subunit assembly to provide a direct route for intercellular communication.

INTRODUCTION

The nexus is a specialized region of contact between the apposed plasma membranes of adjacent cells. Nexuses mediate a type of cell-to-cell communication by providing a route for the direct passage of small molecules between the interiors of the cells (1, 2, 13, 15, 23, 31, 39, 55). Thin-sectioning techniques have produced a variety of images of nexus substructure. Depending on the choice of tissue fixation and staining procedures, nexuses may appear to consist of three layers (50), five layers (13, 20, 30, 62), or seven layers (7, 60). Recently, nexus membranes have been observed to contain arrays of globular subunits in standard thin sections (62), in thin sections containing special tracers (60), by negative staining (3, 25), and by freeze-cleaving (8, 37, 43).[1] However, the interrelationship of the electron microscopic images of the nexus with different preparative techniques remains unclear. The purpose of this study is to attempt to integrate the thin-section and freeze-

[1] The freeze-cleave technique is commonly referred to as "freeze-etching" by many authors, regardless of whether the basic procedure of freezing and cleaving the tissue is followed by an ancillary heat "etching" step. In this paper, the technique will be referred to by the general term "freeze-cleaving," and etching will be specifically mentioned when it is utilized.

cleave images of the nexus. A preliminary report of this work has been presented elsewhere in abstract form (44).

MATERIALS AND METHODS

Tissues

Both thin-section and freeze-cleave techniques were used to examine the myocardium of male and female Charles River mice, guinea pigs, and domestic cats of various weights and ages. Also, the cells were studied in the intermediate zone of the stratified squamous epithelium of the normal human cervix, obtained by 3 mm punch biopsy from several normal patient volunteers of reproductive age.

Thin Section Technique

Tissues were fixed for 2–4 hr at room temperature in 2% glutaraldehyde–2% paraformaldehyde in 0.1 M sodium cacodylate buffer, pH 7.4, 0.05 M in calcium chloride (modified from Karnovsky, 28). After rinsing in 0.1 M cacodylate buffer, we fixed the specimens in 1% osmium tetroxide 0.1 M cacodylate buffer for 4 hr. Some of the tissues were then placed in 0.5% uranyl acetate in Veronal buffer, pH 5.0, for 1 hr (18, 32). The specimens were dehydrated in a series of cold alcohols and embedded in Epon 812 (40) (Shell Chemical Co., New York).

The lanthanum hydroxide tracer technique of Revel and Karnovsky (60) was used to demonstrate nexus substructure in thin sections. A 4% lanthanum nitrate stock solution was adjusted to pH 7.4–7.6 by slowly adding 0.05 N sodium hydroxide with vigorous stirring. The final solution was distinctly opalescent but not flocculent. The lanthanum stock solution was incorporated into the fixative and buffer wash solutions to give a final concentration of 1% lanthanum hydroxide.

Freeze-Cleave Technique

Both fixed and unfixed specimens were examined by freeze-cleaving. Unfixed 1–2 mm tissue blocks were glycerinated by sequential immersion in cold 10, 20, and 40% glycerol solutions containing 0.9% sodium chloride. Other specimens were chemically fixed, prior to glycerination, by immersion for 15-min in 2% glutaraldehyde in 0.1 M cacodylate buffer, pH 7.4, 0.05 M in calcium chloride. Following fixation, the specimens were glycerinated by immersion in 15 or 20% glyercol solutions containing 0.9% sodium chloride.

Two freeze-cleave and etch methods were used for this study. The two methods differ in that method I uses a simple cold block device in which the specimen is cleaved in a bath of liquid nitrogen (9, 11, 69), and method II uses a cryomicrotome to cleave the frozen specimen in vacuo (47–49). We find that results obtained with the two devices are comparable.

METHOD I: A Bullivant type II freeze-cleave device was modified to allow for controlled heat-etching (9, 69). The device was used in a Kinney PW 400 evaporator equipped with a cold trap (Kinney Vacuum Co., Boston, Mass.). In nonetch experiments, specimens were cleaved under liquid nitrogen (−196°C), and replicated with platinum and carbon (46) at −180°C or below. For heat-etching, specimens were cleaved under liquid nitrogen and warmed in vacuo to either −105° or −100°C in 10 min. Specimen temperatures were monitored on a DC recording potentiometer (Bristol, Model 560; Bristol Div., American Chain & Cable Company, Inc., Waterbury, Conn.) by using an Ohmic AC reference junction (Ohmic devices, New York) in place of an ice bath. Replicas were cast in a vacuum of approximately 5×10^{-6} mm Hg within 1 min of the time the heating element was disconnected. Tissue was digested in Chlorox and the replica was rinsed in distilled water and picked up on formvar-coated grids for examination in a Siemens Elmiskop I electron microscope. In method I, specimens were frozen in small stainless steel cartridges (69). On the basis of comparative studies of the size of ice crystals in specimens, it was concluded that freezing rates achieved in methods I and II were essentially identical (unpublished observation).

METHOD II: A Balzers 360 Freeze-Etch machine (Balzers, Palo Alto, Calif.) was used according to the technique described by Moor (46, 47, 59). Small blocks of tissue were mounted on gold-alloy specimen holders (Balzers, Palo Alto, Calif.) and frozen in liquid Freon 22 at −150°C (E. I. du Pont de Nemours & Co., Inc., Wilmington, Del.). The tissue was cleaved at −100°C in vacuo, heat-etched for 1 or 2 min at −100°C, and replicated with platinum and carbon (46). Replicas were washed and retrieved as in method I. Figs. 6 and 14 are replicas prepared with the Balzers device; the remainder were produced by method I.

Photography

Thin sections and replicas were photographed in a Siemens Elmiskop I electron microscope at 60 or 80 kv with 50 μ objective apertures. Micrographs of replicas are printed as positives so that accumulations of platinum appear dark, and shadow regions, devoid of platinum, appear white. For orientation, encircled arrows on micrographs of replicas indicate the direction of shadowing.

RESULTS

Cell-to-Cell Contacts in Myocardium and Cervix

The myocardial cells of mouse, guinea pig, and cat cardiac muscle are long cylinders which branch and are attached to each other end-to-end at intercalated discs (Fig. 1) (19, 20, 42, 50, 51, 63). At an intercalated disc, the plasma membranes of adjacent cells are interdigitated, giving rise to segments of the plasma membrane which lie parallel to the axis of the myofilaments (longitudinal segments) and segments perpendicular to this axis (transverse segments). The intercalated disc segments contain three types of junctional specializations: fasciae adherentes, maculae adherentes (desmosomes), and nexuses ("gap" junctions). The fasciae adherentes are found on transverse segments, attach the myofilaments to the plasma membrane, and are the predominant form of intercellular junction responsible for the end-to-end adhesion of the cells. Maculae adherentes and nexuses are on the longitudinal segments of the disc (Fig. 1).[2] At either a macula or a fascia adherens, the plasma membranes are separated by 300 A of extracellular space containing a rather amorphous proteinaceous material. At a nexus, the adjacent plasma membranes appear to come into very close apposition (Fig. 1).

A detailed description of the cervical epithelial cell surface is the subject of a separate communication (McNutt, Hershberg, Weinstein, data in preparation); general features of the ultrastructure of the epithelium have been recently reviewed by Hackemann et al. (26). The human cervical epithelium can be divided into three zones: basal, intermediate, and superficial. Particular attention is paid in this study to the intermediate zone where nexuses are present in the greatest numbers. The cells of the intermediate zone are large, measuring 30–40 μ in diameter, and have hundreds of finger-like processes at their cell surface. The processes of adjacent cells are often closely apposed and attached side to side by maculae adherentes and nexuses. The maculae adherentes are more highly developed in cervical epithelium than in the myocardium. The proteinaceous material in the 300 A interspace at a macula adherens has a more distinct central dense stratum in the cervix than in myocardium (29). Further, there is a heavier condensation of filamentous material in the cytoplasm adjacent to the membrane of maculae adherentes in cervical epithelium. Nexuses of cervical epithelium resemble those of myocardium, except for their extent. The cervical nexus is typically a small, round to oval area of contact less than 1 μ in greatest diameter.

Nexus Ultrastructure in Thin Sections

The appearance of a nexus in thin sections is related to the fixation and staining procedure used during tissue preparation. The different appearances of the nexus are mainly due to the apparent number of layers which form the nexus. In contrast, the over-all thickness of nexus is constant, 180 $\pm$ 10 A, with the various fixation and staining methods.

Nexuses may have a three-layered, five-layered or seven-layered appearance in sections (Figs. 2–5). When tissue is fixed with osmium tetroxide alone and the sections are stained with lead citrate, the nexus has a three-layered appearance (i.e. dark-light-dark), since intense staining is achieved only at the inner (juxtacytoplasmic) surfaces of the plasma membrane (50). The nexus has a five-layered appearance (Fig. 2) in tissue fixed in potassium permanganate (13, 14, 62), in osmium tetroxide, or in aldehyde-osmium tetroxide with subsequent staining of sections with uranyl acetate (30) and lead citrate (20, 42). However, fixation of tissue either with osmium tetroxide or aldehyde-osmium tetroxide and staining of the tissue blocks with uranyl acetate before dehydration results in a seven-layered nexus (7, 60) (Fig. 3). This seven-layered appearance can be converted to a five-layered one by intense staining with lead citrate (compare Figs. 2 and 3). The central electron-lucent zone of the seven-layered complex is 20–30 A in thickness and appears to be continuous with the extracellular compartment (60). Since this central lucent zone suggests a "gap" separating the nexus membranes, some workers have referred to this type of junction as a "gap junction" (7, 25, 59).

Use of the colloidal tracer, lanthanum hydroxide, provides additional information about nexus ultrastructure (7, 41, 60). Our results with

[2] Owing to the complex interdigitation, many segments of the plasma membrane are oblique to the myofilament axis. Oblique segments may contain any of the three intercellular junctions, but the myofilaments insert only into fasciae adherentes (42).

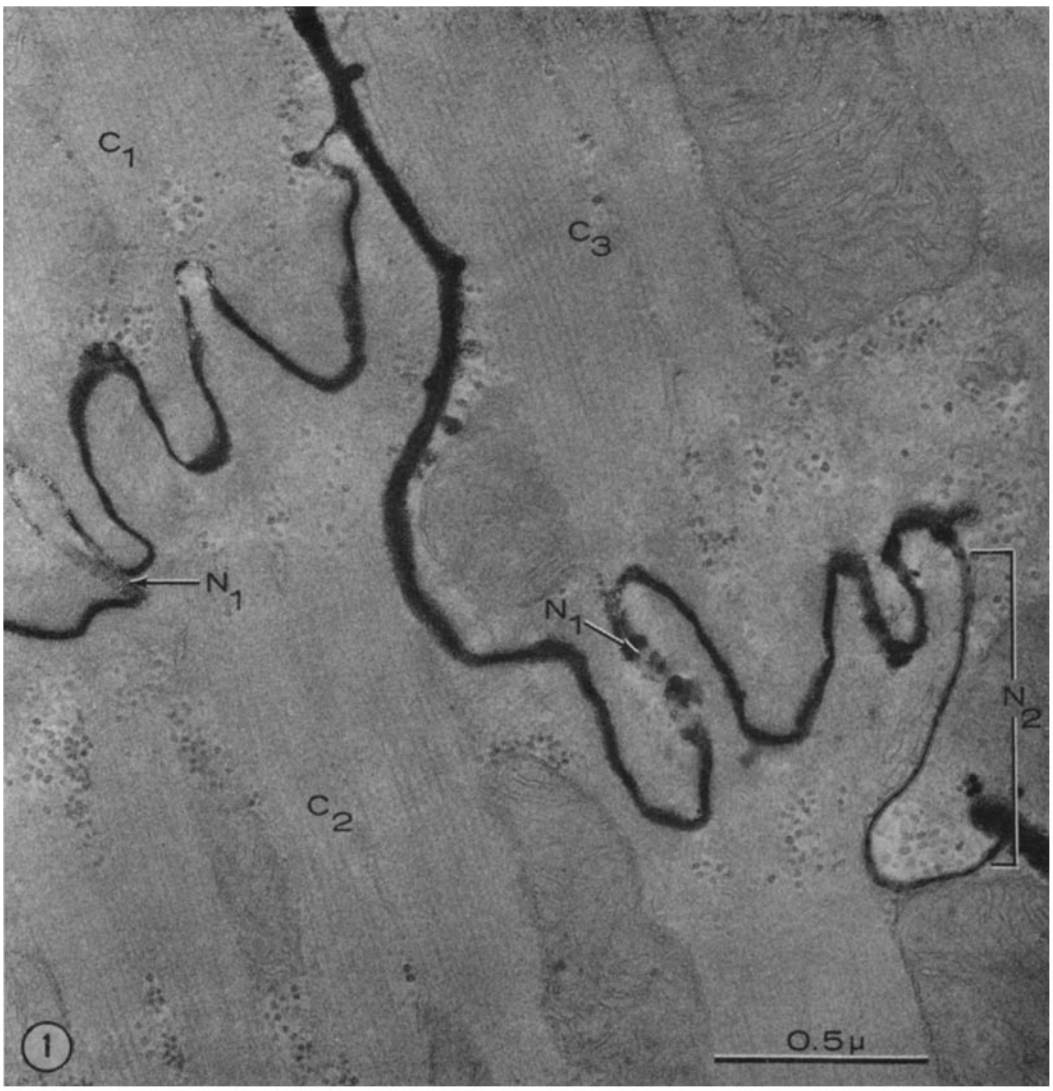

FIGURE 1 Thin section of an intercalated disc as outlined by the electron-opaque tracer lanthanum hydroxide. This micrograph illustrates the area of attachment of three myocardial cell processes (C_1, C_2, and C_3). The lanthanum tracer fills the intercellular space and outlines the interdigitations of the adjacent cell borders. At nexuses, the lanthanum penetrates the central region of the junction in a characteristic manner (Figs. 2–5), a feature useful for demonstrating that frequently small nexuses (N_1) and an occasional large nexus (N_2) are present on the longitudinal segments of plasma membrane at the intercalated disc.

Glutaraldehyde-OsO_4 fixation, *en bloc* lanthanum tracer, section stained with 0.05% lead citrate.
× 56,500.

lanthanum tracer are in general agreement with those of Revel and Karnovsky (60), who first reported its use as a passive tracer in mouse myocardium. Certain features of the structures revealed by lanthanum deserve to be reemphasized, and the ultrastructure of lanthanum-impregnated nexuses in the cervix are reported in detail for the first time (Figs. 4 and 5). The

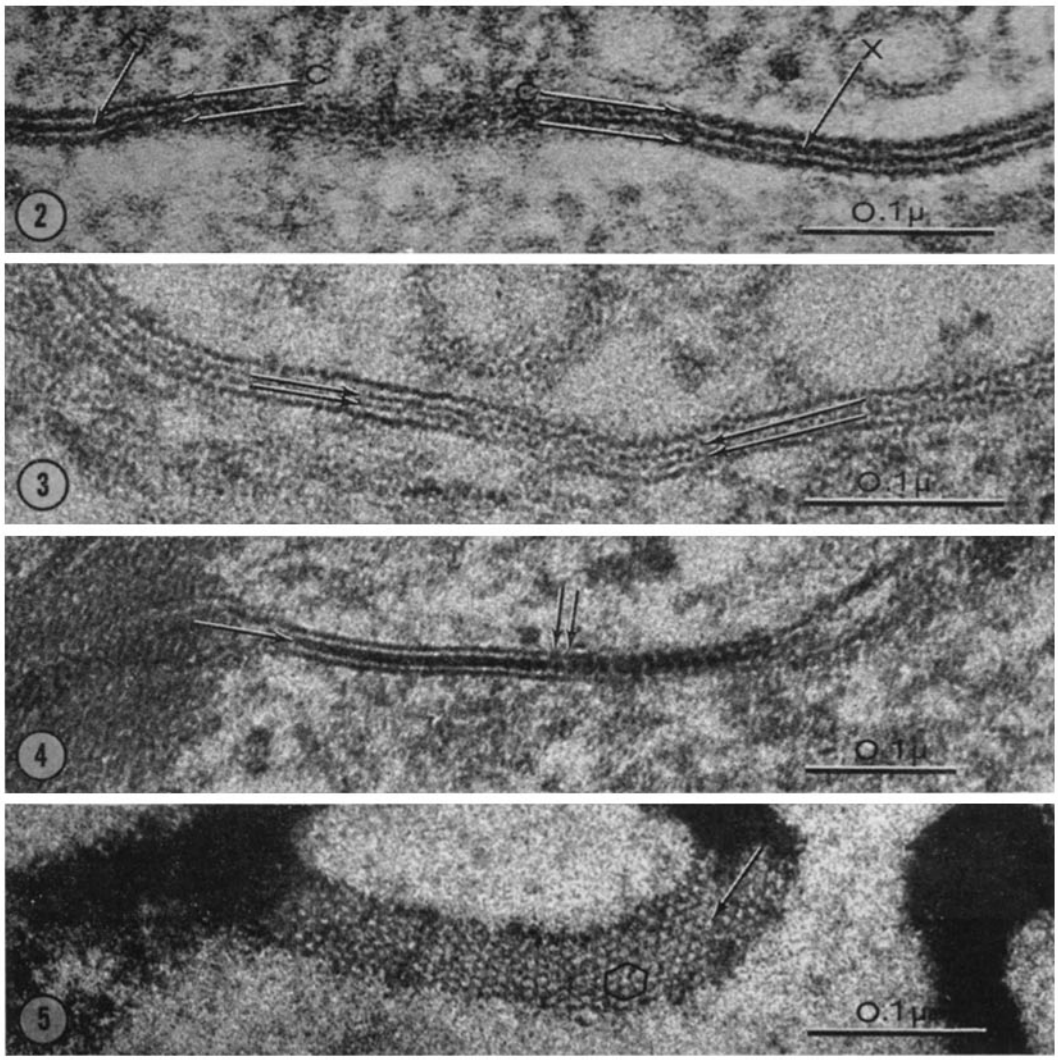

FIGURE 2 Five-layered nexus at high magnification. This nexus has two 55 A dense juxtacytoplasmic layers (*c*) and a central 40 A dense layer (*x*). Two paramedian 20 A electron-lucent zones separate the three dense layers. This appearance is typical of nexuses prepared with a variety of fixation and staining procedures. Myocardium, aldehyde-OsO_4 fixation; *en bloc* uranyl acetate, on section 0.3% lead citrate stain × 250,000.

FIGURE 3 Seven-layered nexus at high magnification. This nexus has a 30 A electron-lucent zone that appears to separate the apposed plasma membranes (double arrows). More intense lead staining often will stain material within the central 30 A zone, obliterating the central lucent zone and converting the seven-layered appearance to a five-layered appearance.
Cervical epithelium, aldehyde-OsO_4 fixation; *en bloc* uranyl acetate, on section 0.05% lead citrate stain. × 260,000.

FIGURE 4 Nexus containing lanthanum hydroxide tracer viewed in transverse section. Electron-opaque lanthanum impregnates a central 60 A region of the nexus (single arrow). The lanthanum impregnates the central lucent zone and at least the two outer leaflets of the apposed plasma membranes in the seven-layered appearance of the nexus. As the junction begins to be tilted in the plane of section (double arrow and to the right), the lanthanum appears interrupted by electron-lucent structures bridging the central region of the nexus.
Cervical epithelium; aldehyde-OsO_4 fixation, *en bloc* lanthanum tracer, on section 0.2% lead citrate stain × 200,000.

FIGURE 5 Nexus containing lanthanum tracer viewed *en face*. The lanthanum fills thin anastomosing channels which course around electron-lucent subunits, 60 A in diameter (at arrow). The subunits often are hexagonally packed (shown in box). Since the subunits themselves have an electron density resembling that of the cytoplasm, they probably connect the two membranes. Cervical epithelium, aldehyde-OsO_4 fixation, *en bloc* lanthanum tracer. × 235,000.

lanthanum tracer freely permeates the extracellular space of fixed myocardium and cervix, and is usually excluded from the intracellular compartment of cells by intact plasma membranes. The lanthanum may, however, penetrate the region of the "outer leaflet" of each "triple layered unit membrane" at the nexus (60).

When lanthanum is present in either myocardial or cervical nexuses, a central electron-opaque stratum, 60–70 A in thickness, is demonstrated in cross-sections (Fig. 4). Thus the lanthanum penetrates the 20 A "gap", plus the outer leaflets of the apposed nexus membranes (compare Figs. 3 and 4). *En face* views of nexuses in sections show that lanthanum has access to a network of thin anastomosing channels, approximately 20 A wide, which course around subunits 70 A in diameter (Fig. 5). The subunits probably span the gap between the two membranes since, if a complete separation of the membranes existed and the intervening space filled with lanthanum, the resulting 20 A layer of electron-opaque lanthanum viewed *en face* would tend to obscure the subunit pattern. Instead, the subunits themselves have an electron density equivalent to that of the cytoplasm. Also, lanthanum occasionally localizes as a dot 15 A in diameter in the center of the subunits (60), suggesting the presence of a central hydrophilic channel in the subunits, although it is not clear how the lanthanum enters this channel.

Freeze-Cleaved Cell-to-Cell Junctions

The interpretations of cytology based on thin sections of myocardium and cervix are in large measure corroborated by freeze-cleaving (Fig. 6). Both maculae and fasciae adherentes can be identified by virtue of the fact that membranes at these junctions are separated by the expected 300 A interspace, and there is an accumulation of filamentous material in the cytoplasm adjacent to the membranes. On the longitudinal segments of the intercalated disc the membranes of adjacent cells appear to come into direct contact, forming specialized regions corresponding in size and location to the nexuses seen in thin-sections. Similar nexuses provide sites of contact between the interdigitated processes of adjacent cervical epithelial cells in the freeze-cleave preparations.

Identity of Fracture Faces

In order to present our results on the substructure of the freeze-cleaved nexus, the current evidence concerning the path of cleavage planes within membranes must be considered on the basis of work from several laboratories. There are two prevalent interpretations in the literature as to where cleavage planes pass in relation to the layers of the trilaminar plasma membrane of thin-sections. Mühlethaler, et al. (49) originally proposed that two cleavage planes might exist, one along the true inner (juxtacytoplasmic) surface of the membrane, and a second along the membrane's true outer surface. Branton (5), on the other hand, suggested that there is a single cleavage plane for most membranes. He believes that membranes are cleaved internally and that the faces revealed by cleavage represent new surfaces which are created during cleavage by separation along some plane within the membrane's interior. Although some early evidence appeared to favor the hypothesis of Mühlethaler et al. (10, 22, 65), more recent evidence strongly indicates that the Branton hypothesis is valid for many membrane systems (53, 54, 56, 57, 66, 67, 70, 71; Bullivant, personal communication). In our judgement, the evidence for the membrane splitting at the nexus is compelling. Our micrographs of nexus membranes are most satisfactorily interpreted in terms of the Branton hypothesis, as will be detailed later.

When a junctional or nonjunctional plasma membrane is freeze-cleaved, it is split into two lamellae, one adjacent to the cytoplasm (lamella 1 or [Lm 1]), and the other adjacent to the extracellular compartment (lamella 2 [Lm 2]). The cleaving process generates two new membrane faces which are apposed to each other within the membrane interior. For descriptive purposes, a convention has developed so that the membrane faces are designated as face A, B, C, or D. The new face of the inner lamella (Lm 1) is oriented towards the extracellular compartment and is called face A. The new face of the outer lamella (Lm 2) is oriented towards the cytoplasm and is face B. Although true inner and outer surfaces of the membrane are not usually revealed by cleaving alone, with subsequent heat-etching true surfaces of the membrane may be revealed

FIGURE 6 Replica of an intercalated disc in the region of fascia adherens of freeze-cleaved and etched myocardium. The cleavage has passed through the cytoplasm of one cell (Cyt_1) and then been deviated by its plasma membrane (M_1). After passing through this membrane (M_1) and across the intercellular space (*IS*), it has been deviated by the adjacent membrane (M_2) before breaking into the cytoplasm of the second cell (Cyt_2). When the fracture plane is deviated by membranes, it cleaves through their interior, thus revealing the inner face of the outer lamella of membrane 1 (*face B*) and the outer face of the inner lamella of membrane 2 (*face A*). These membrane faces are studded with small particles. The cytoplasm appears granular in this heat-etched preparation. Encircled arrow indicates direction of platinum shadowing. × 62,500.

(5, 53, 54, 56, 57, 66).[3] The true juxtacytoplasmic surface of the membrane inner lamella (Lm 1) is designated face C. The true outer surface of the outer lamella (Lm 2) is face D. Thus, the inner lamella (Lm 1) has a face C and a face A; the outer lamella (Lm 2) has a face B and a face D. In near cross-fractures of nonspecialized plasma membrane, the sides of these two lamellae appear as narrow parallel ridges, each about 40–50 A in thickness.

In this study, freeze-cleaving the nonjunctional regions of the plasma membrane of myocardial and cervical epithelial cells reveals a face A (Fig. 7) and a face B (Fig. 8) which are studded with many 60–100 A particles. As is typical of many plasma membranes, face A has approximately 4–5 times as many particles as face B (6, 58, 69). A few depressions are found on membrane faces A and B, but the total number of depressions is insufficient to have accommodated all of the particles seen projecting from the membrane faces (5). Although the particles are not generally visualized in thin sections of the plasma membrane, the particles are a finding consistent for each membrane type, and are thought to reflect actual membrane components (5, 6, 24, 69).

Ultrastructure of Freeze-Cleaved Nexus Membrane

Since the nexus is constructed of two apposed plasma membranes, a cleavage may reveal aspects of either or both of the plasma membranes forming the nexus. There are actually three paths which the cleavage plane may follow. First, the cleavage may enter the potential cleavage plane (*PCP*) of only one of the two apposed membranes (Fig. 9). With this cleavage, the internal structure of one membrane is demonstrated, while its partner membrane is not apparent at the fracture face. Secondly, the cleavage may pass in a stepwise fashion from the potential cleavage plane in the interior of one membrane into the potential cleavage plane in the interior of the adjacent membrane. This cleavage reveals aspects of the internal structure of both membranes in the same fracture face. Thirdly, the cleavage may pass directly through the nexus, revealing it in cross-fracture, and showing none of the membrane faces. Cleavages reveal either the face A or B of the nexus membranes if the cleavage plane enters the potential cleavage plane of one of the membranes. The failure of the cleavage plane to reveal a face C or D at the nexus is probably the result of the tendency of the cleavage to remain within one or the other membrane, instead of fracturing along their outer surfaces. The face C of the nexus membranes can be revealed by heat-etching, but the face D of the membrane at the nexus has not been demonstrated. The failure of heat-etching to reveal a face D at the nexus indicates that the two membranes are in contact at this face with no etchable space detectable between them with the freeze-cleave techniques employed. In nexuses where both faces A and B have been revealed, there is a constant relationship between the two faces. Nexus face B is always visualized on a layer which rests on top of another membrane layer having nexus face A. This relationship is produced by cleaving first the potential cleavage plane of one membrane and then the other, thereby revealing face B of one membrane and face A of the other membrane (Figs. 9-12). The nexus faces A, B, and C are seen to be continuous with the surrounding nonjunctional membrane faces (Figs. 10-12).

With or without chemical fixation, the nexus face A exhibits a closely packed array of particles which are 50-75 A in diameter, as measured in replicas, in the plane of the membrane (Figs. 10 and 11). Much of the variability in size can be attributed to variations in the thickness of different replicas, since the particles are usually of rather uniform size in a given replica. The height of the particles is difficult to estimate but is probably in the neighborhood of 50 A. In high quality replicas, central depressions 20 A in diameter can be visualized on the tops of many of the nexus face A particles (Fig. 12, insert). It has not been possible to estimate the depth of these central depressions in the face A particles, but it is possible that these depressions represent the position of a channel or pore through the membranes (see Discussion).

Analysis of the electron microscopic images of nexus face B is complicated by the fact that this face can have two distinctive appearances. One

[3] Heat-etching involves exposing the cleaved surface of the specimen to high vacuum at temperatures in the neighborhood of −100°C. Under these conditions, volatile components such as ice sublime away. Where ice abuts against the membrane at the fracture face, the removal of ice by sublimation reveals the membrane surface.

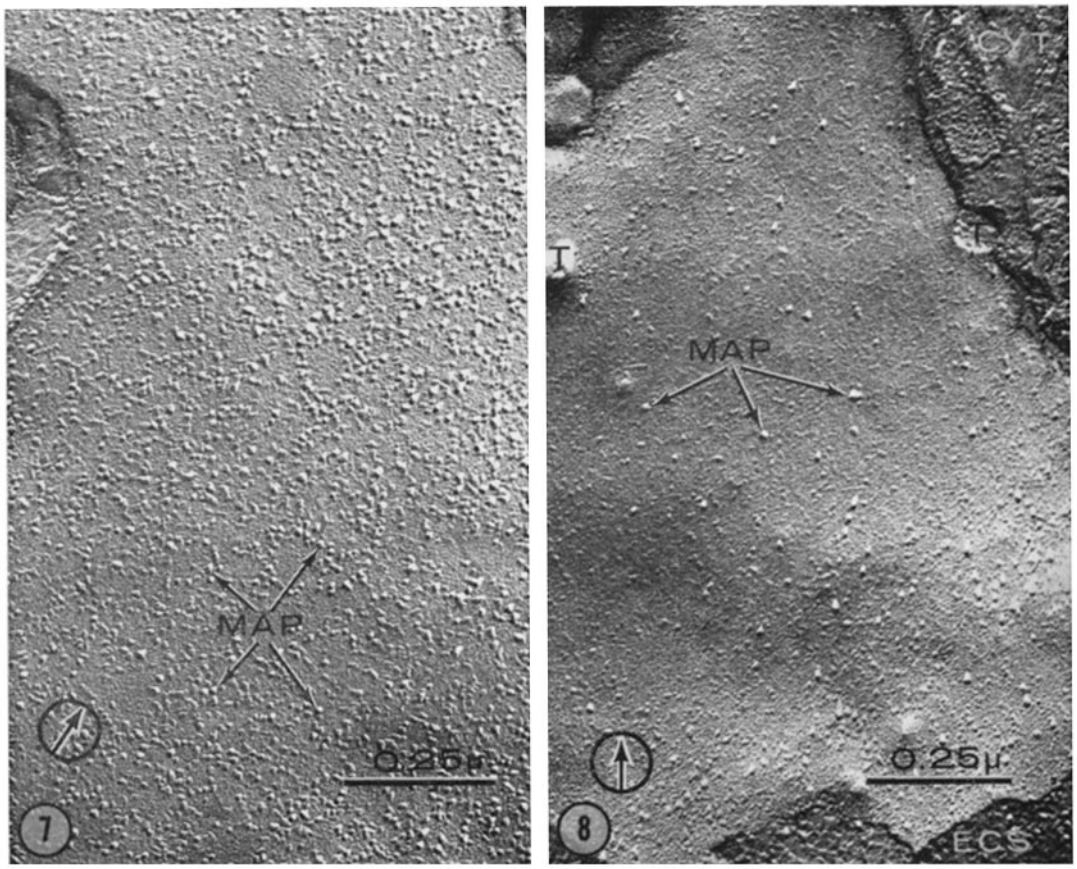

FIGURE 7 Face A of mouse heart nonjunctional plasma membrane (sarcolemma). The outwardly directed face of the plasma membrane is studded with 60–100 A membrane-associated particles (*MAP*). Encircled arrow indicates direction of platinum shadowing. × 78,000.

FIGURE 8 Face B of mouse heart sarcolemma. This inwardly directed face of the plasma membrane has fewer 60–100 A particles (*MAP*) on its surface. In the intervening areas of membrane, the surface is finely textured. The orifices of two T tubules (*T*) are present. A small amount of extracellular space (*ECS*) and cytoplasm (*Cyt*) are shown. Encircled arrow indicates direction of platinum shadowing. × 76,000.

appearance of face B is most strikingly evident when the platinum shadowing is at a high angle of incidence, whereas the other is demonstrated only with low angle shadowing. Since nexuses are frequently incorporated into curved regions of the plasmalemma, areas of both high-angle and low-angle shadowing may appear in replicas of a single nexus. Where nexus face B is shadowed at a high angle, the face appears studded with pits measuring 30–40 A in diameter (Figs. 10 and 11). These pits may be hexagonally arrayed with a 90-100 A center-to-center spacing, although this precise ordering is less prominent at some nexuses. When the face B pits are most distinct, the remainder of the nexus membrane face B appears smooth. On the other hand, at low shadowing angles, the 30-40 A pits are often not apparent; instead, face B of the nexus has a patterned cobblestone appearance, suggesting closely packed subunits forming a continuous sheet. These subunits ("cobblestones") appear to be 90-100 A in diameter when viewed *en face*, and are estimated to be approximately 35 A in height, on the basis of observations described below in the section on nexus cross-fractures. Another aspect of the closely packed subunits is

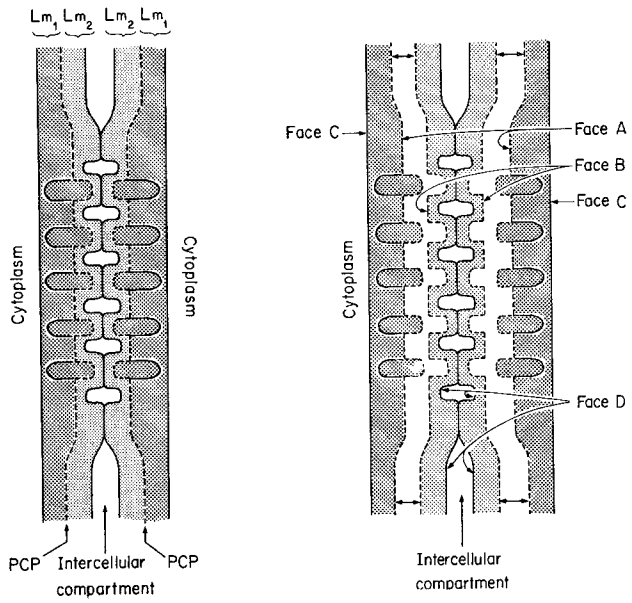

FIGURE 9 This diagram illustrates the various membrane faces of the nexus as seen in freeze-cleave and -etch preparations. On the left, the nexus is shown as composed of two membranes, each of which is made up of two lamellae (*Lm*$_1$ and *Lm*$_2$). These two lamellae can be separated if a cleavage passes through the potential cleavage plane (*PCP*) in the interior of the membrane. On the right, the nexus has been split in the two likely cleavage planes and the locations of the *Face A*, *Face B*, *Face C*, and *Face D* are shown. *Face C* can only be revealed by etching and *Face D* has not been demonstrated at a nexus, indicating that the membranes are in contact at this level. This diagram is not drawn to an exact scale.

demonstrated where Lm 2 is cross-sectioned. In such regions, Lm 2 has a serrated edge. The bulges which create the serrated appearance are interpreted as representing sides of Lm 2 subunits, and the grooves are interpreted as representing the intersections between adjacent globular subunits. In contrast, in a cross-fracture through a nonjunctional region, the side of Lm 2 usually appears smooth. A third image of Lm 2 is encountered where fortuitous microfractures chip clusters of subunits out of Lm 2 and leave individual subunits stranded behind (Fig. 12, insert). When such an isolated subunit is appropriately shadowed, a small pit or depression can be seen at its face. Also, in the intervening areas between the extremes of high-angle and low-angle shadowing, there are transitional zones that produce images which suggest that the pits are centrally placed in the face B subunits. The central pit in the face B subunit may represent a segment of a transmembrane hydrophilic channel (see Discussion).

An additional feature of the nexus faces A and B is that there is usually a thin rim of smooth membrane face which encircles the nexus and represents the transitional region from general plasma membrane to nexus membrane (Fig. 13). It is possible that this smooth rim represents membrane specialization, but it is also possible that the rim is a region where the path of the cleavage plane changes levels when passing from general plasma membrane to nexus membrane.

When unfixed tissue specimens are allowed to stand at 4°C in glycerol solutions, the particles of nexus face A and the pits of nexus face B tend to lose their hexagonal ordering. Loose clusters of particles on face A and pits on face B become separated by irregular zones of flat smooth membrane.

Heat-etching is useful in some applications of the freeze-cleave technique. Nexus faces A and B are essentially nonetchable and have identical appearances either with high quality etching or without etching. However, poor quality etching[4]

[4] Poor quality etching can be identified by the appearance of structural alterations at the fracture face which cannot be directly related to the sublimation of water from the face. Some artefacts can be ascribed to the recondensation of water onto the nonetchable surfaces of the fracture face.

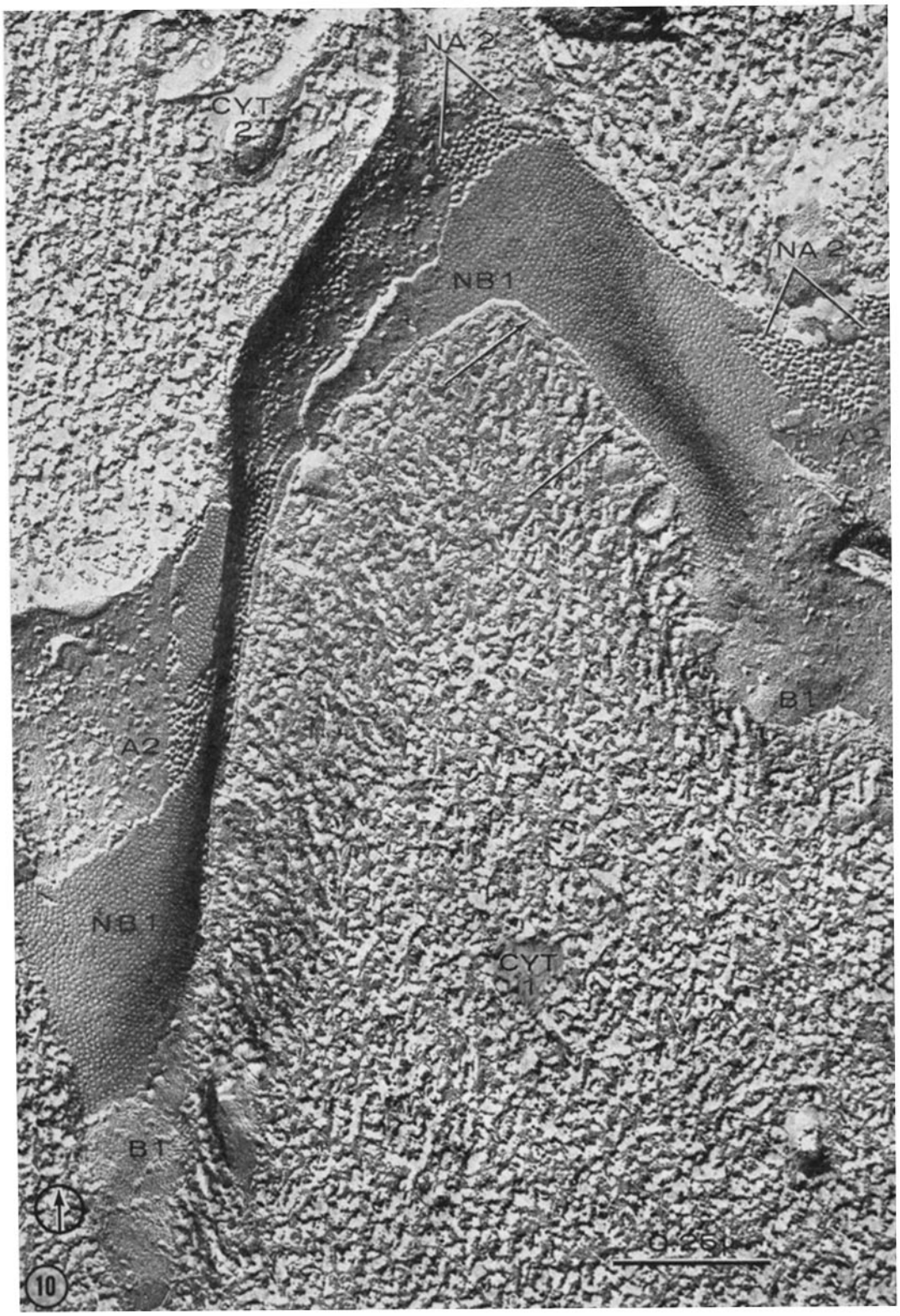
NA 2
CYT 2
NB 1
NA 2
A2
B1
A2
NB 1
CYT 1
B1
0·2 μ
10

can produce several artefacts in nexus faces A and B, such as apparent aggregation of the particles of face A into small groups and obliteration of the pits of nexus face B.

Nexus face C, the juxtacytoplasmic surface of the nexus, is not visualized as a fracture face, but can be exposed by heat-etching (Figs. 12, 14, 15). Face C has a granular texture and is without distinctive patterning. Face C patterning may be obscured by a thin coating layer of nonsublimable eutectic, originating from the adjacent cytoplasm during freezing, which might then be demonstrated on the face by heat-etching. The thickness of the membrane lamella bearing face C is approximately 70 A. The side of the lamella bearing nexus Face C occasionally contains a distinct particle 60–100 A in diameter.

Nexus Cross Fractures

In etched preparations, the nexus frequently is seen in near cross-fracture as three parallel ridges with an overall thickness of 200–220 A as measured in replicas (Figs. 9, 16–21). Each of the juxtacytoplasmic ridges is approximately 70 A in thickness and is interpreted as representing the inner lamella (Lm 1) of each membrane at the nexus. The central 70 A ridge corresponds to the joined outer lamellae (Lm 2-Lm 2) of the two apposed membranes. Therefore, subunits in each sheet (Lm2) would be 35 A in height. The most accurate measurements of ridge thickness are made on regions of the nexus where the fracture has produced a relatively smooth cross-section which would be subject to less shadowing distortion than a very irregular region of the cross-section. Also, these measurements must be made in areas of the specimen where rapid freezing has produced extremely fine ice crystals, some of which can be assumed to lie in contact with the membrane surface. Etching then reveals the actual nonetchable thickness of the nexus membranes.

DISCUSSION

It is widely held that the trilaminar thin-section appearance of biological membranes (61) fails to provide a morphologic basis for transmembrane transport (34). Electron microscopists have investigated specialized regions of biomembranes where a transport function might be more important than the barrier function of membranes. One of the best examples of such a specialization is the region where the plasma membranes of heart muscle cells come into direct contact providing for electrical coupling of the cells. Sjöstrand et al. (63) first visualized these regions of contact, and later Karrer (29, 30) recognized their probable function. At these contacts, the two membranes of adjacent cells came into such close apposition that the outer dense lamina of each of the membranes could only be resolved as a single dense lamina in the center of the junction. Therefore, the junction of two triple-layered "unit" membranes had the appearance of a five-layered membrane complex. In 1962, Dewey and Barr (13) observed similar five-layered complexes connecting smooth muscle cells, and suggested that electrical coupling of smooth muscle cells occurs at these sites. They used the word "nexus" (*L.* connection) to designate such junctions. The next contribution to the elucidation of the morphology of these junctions was made by Robertson (62) who reported that five-layered junctions formed the electrical synapses of Mauthner cells in gold fish brain, and that these junctions included distinct subunits as one of their com-

FIGURE 10 Intercalated disc of mouse heart showing two nexuses. This replica reveals that the cleavage plane has passed from the cytoplasm (Cyt_1) of one cell and has been deviated by its plasma membrane revealing *face B* (B_1—nonjunctional *face B*; NB_1—nexus *face B*). After breaking through the membrane, the cleavage plane passes to the plasma membrane of the second cell, revealing *face A* of the membrane. (A_2—nonjunctional face A; NA_2—nexus face A). The cleavage then passed through membrane 2 and into the cytoplasm (Cyt_2) of cell 2. Nexus face B (NB_1) is continuous with nonjunctional membrane face B (B_1), but, instead of having the scattered particles on membrane face B (B_1), nexus face B (NB_1) exhibits a closely packed array of discrete depressions. Where nexus face B has been cleaved away, the underlying nexus face A is revealed. The two membranes appear in contact at the nexus. Heat-etching of this preparation has revealed the ridge (at arrows) representing the lamella cleaved away from nexus Face B. The juxtacytoplasmic lamella would have the nexus Face C (not shown). Encircled arrow indicates the direction of platinum shadowing. ×100,000.

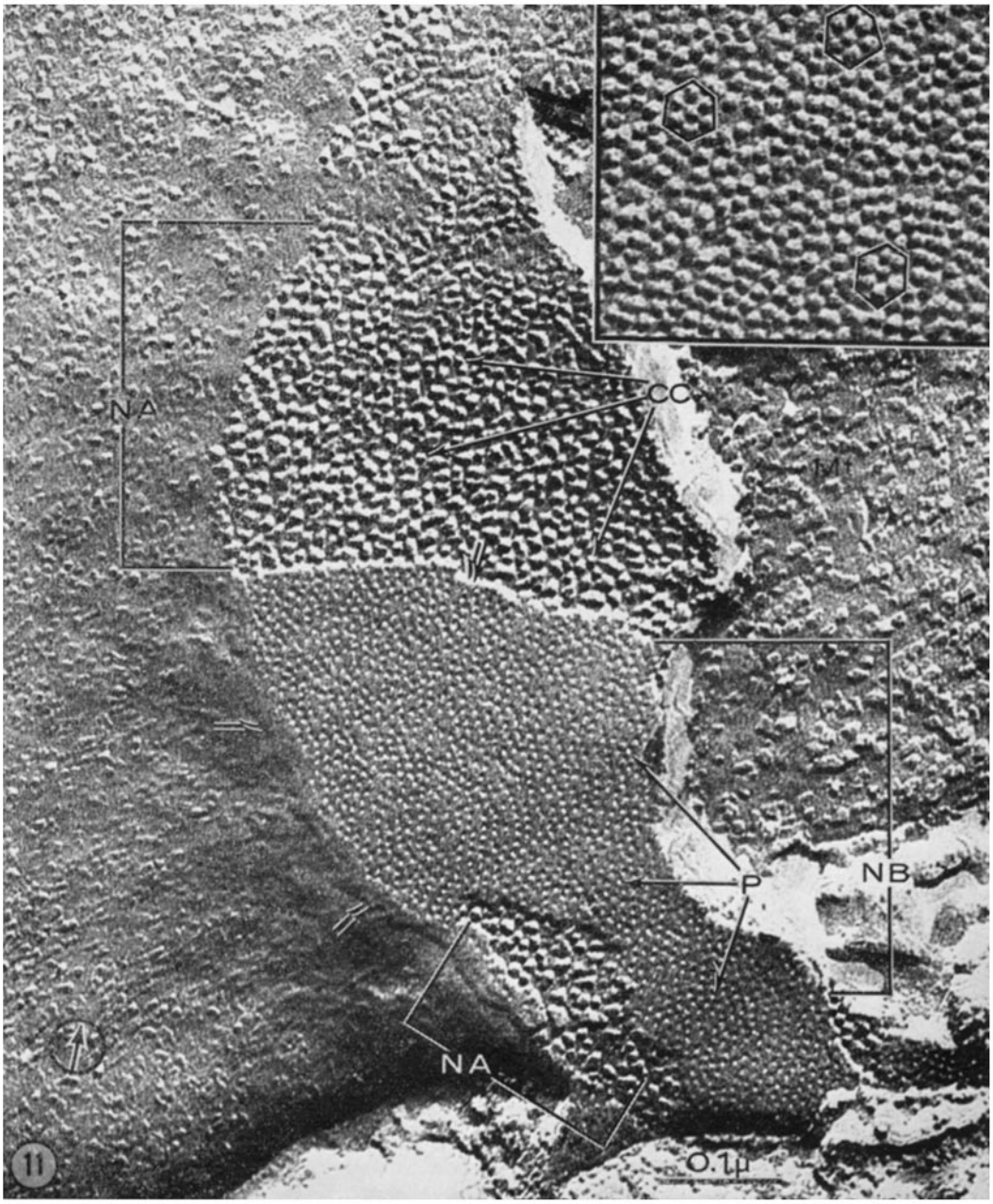

FIGURE 11 *En face* view of a small nexus in freeze-cleaved and -etched myocardium. Nexus face B (*NB*) contains closely arrayed pits (*P*) 35–50 A in replica diameter. The edge of nexus face B is marked with double arrows. Protruding from nexus face A (*NA*) are many particles, "contact cylinders" (*CC*), which are better resolved in the insert (*P*, particles). Encircled arrow indicates the direction of platinum shadowing. × 170,000. Insert: Nexus face A at high magnification. The face A particles are of uniform size and frequently form hexagonal arrays (in boxes). × 220,000.

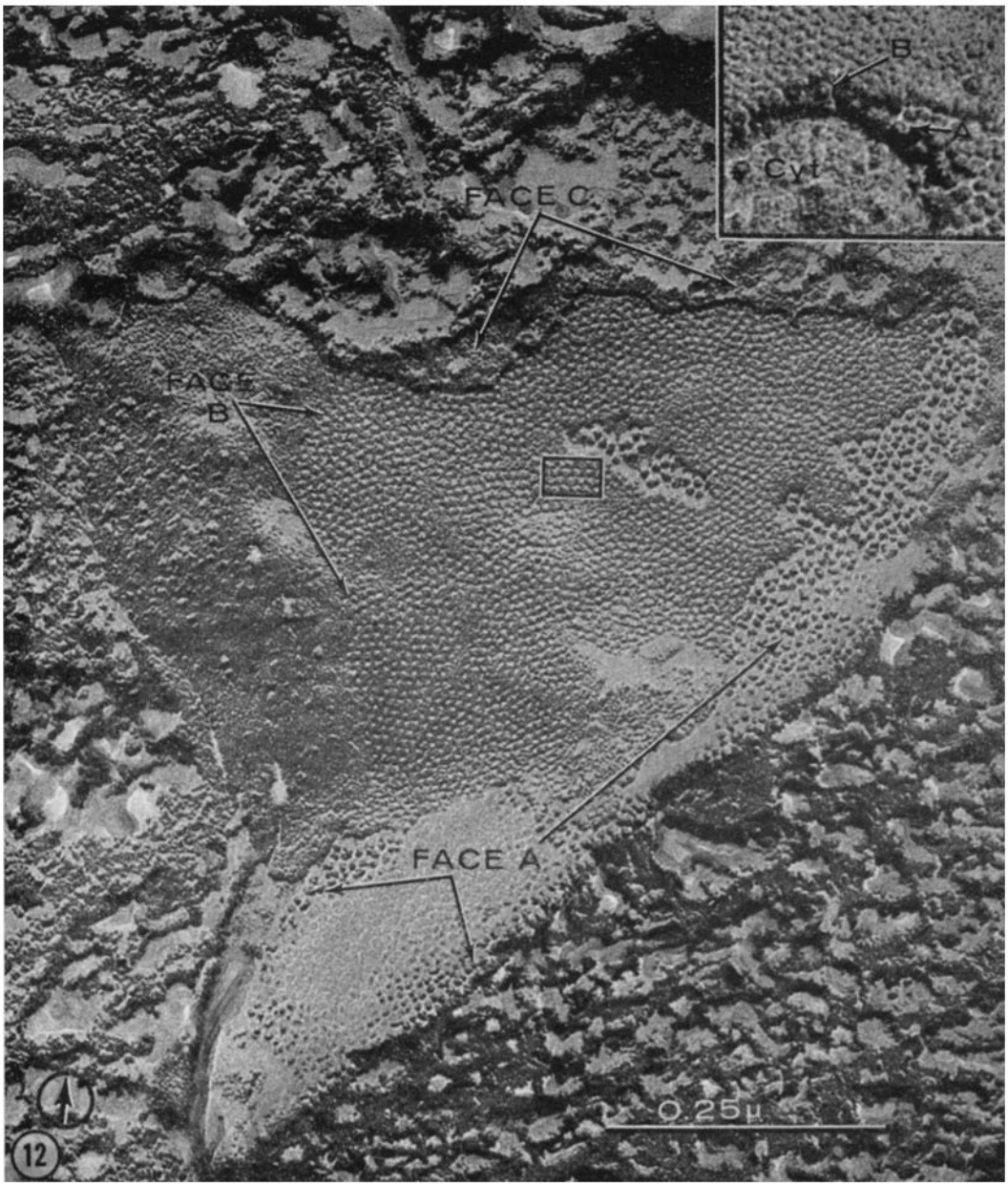

FIGURE 12 Nexus in extensively heat-etched myocardium. Three layers are revealed by cleaving and etching the nexus, and each layer has a distinctive face appearance. Nexus *face A* is here shown at very low angle shadowing with the "contact cylinders" casting long shadows. On top of this layer is another layer having the nexus *face B* appearance. The lower left portion of face B has the typical hexagonal array of pits. Where curving of the nexus produces lower angle shadowing on face B, the surface of face B takes on a patterned cobblestone appearance suggesting subunits (in box). On top of this middle layer is another layer which shows a small area of face C that reveals no ordered structure in this type of preparation. Encircled arrow indicates the direction of platinum shadowing. × 155,000. *Insert*: Very high magnification of a replica of a nexus which has been shadowed at a low angle. A subunit (*B*) of nexus face B is visible with a central pit which may represent the location of a central hydrophilic channel. Several of the subunits of face B previously adjacent to this particular subunit have been cleaved away, leaving it relatively isolated. The nexus face A is present on a level below the face B. A particle (*A*) of nexus face A shows a central pit. A small area of adjacent cytoplasm (*Cyt*) can also be seen. × 250,000.

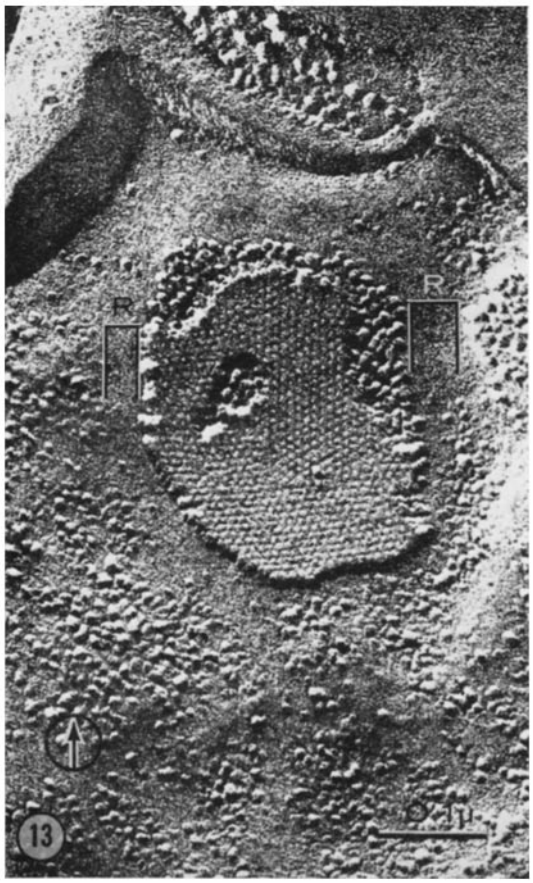

FIGURE 13 Small oval nexus in freeze-cleaved myocardium. An isolated segment of the nexus face B rests on the underlying face A. The narrow rim of smooth membrane face (*R*) may correspond to a region where the level of the cleavage plane changes from its usual central position in nonjunctional membrane to the asymmetric level at the nexus. Encircled arrow indicates the direction of platinum shadowing. × 110,000.

ponents. Robertson visualized *en face*, polygonal subunits that were often hexagonally packed, but he was unable to localize these subunits precisely within the membrane complex because of limitations imposed by thin-sections. However, on the basis of analysis of the micrographs of electrical synapses at various degrees of tilt, he tentatively concluded that the pattern he observed could be produced by polygonal subunits contained within the apposed outer leaflets of the two membranes (62).

Another type of junction bears mention here, since it is frequently confused with the nexus. At the apex of simple columnar epithelial cells, Farquhar and Palade (16) found five-layered junctional complexes which form a belt-like seal around the cells and prevent free diffusion across the epithelium. They called these five-layered junctions "tight junctions" or zonulae occludentes. Since the five-layered junctions described by Karrer (30) and Robertson (62) were not belts of membrane-to-membrane "fusion" encircling the cell but were small, spot-like connections, the term "maculae occludentes" was proposed by Farquhar and Palade (17, 18) for these junctions.

Later, several consistent differences were noted in the ultrastructure of these two kinds of junctions. In over-all thickness, the zonulae occludentes of Farquhar and Palade are less than twice the thickness of the "unit" plasma membrane, whereas the junctions responsible for electrical coupling are usually 2–2.5 times the thickness of the plasma

membrane in aldehyde- and/or osmium tetroxide–fixed tissue (7).[5] Further, Revel and Karnovsky (60) found that staining with uranyl acetate before dehydration produced a seven-layered appearance at the nexus by revealing a central 20–30 A electron-lucent zone, which accounts, in part, for the nexus having a greater over-all thickness than the "tight" junction. They further showed that the central zone of the nexus was partially permeable to extracellular tracers such as colloidal lanthanum hydroxide (60). Revel (59) suggested that the nexus be called a "gap junction" to distinguish the nexus from the tight junction. In nexuses permeated with lanthanum hydroxide and viewed *en face*, Revel and Karnovsky (60) also revealed a hexagonally packed array of subunits, similar in center-to-center spacing to those seen by Robertson (62). Similar arrays have been demonstrated with negative staining (3, 25) although, as with thin-sections, the image seen with negative staining only relates to the configuration of the outermost surfaces of membranes, and does not elucidate the relation of the apparent subunits to the membrane internal structure (53, 54). In this study, the array of subunits revealed by lanthanum has been confirmed in mouse myocardium, and has also been observed in both the myocardium and the cervical epithelium of other species.

Faces Revealed by Freeze-Cleaving

The freeze-cleave technique was first applied to the study of nexus ultrastructure by Kreutziger who, in a preliminary report (37), described two distinctive fracture faces for aldehyde-fixed nexuses. One face, which he interpreted as the true outer surface of a nexus membrane, was covered with a hexagonal array of small particles, and the second face, interpreted as membrane inner (juxtacytoplasmic) surface, had a similar array of small pits. Additional faces revealed by heat-etching were not described. McNutt and Weinstein (43) described comparable arrays in nexuses of unfixed tissue.

The hypothesis that the membrane's true outer and inner surfaces are revealed by freeze-cleaving was originally proposed by Mühlethaler et al. (49). This interpretation was previously accepted by ourselves (10, 22, 43, 69) and many others (33, 47); however, it has now been invalidated by double replica and surface labeling experiments. In double replica experiments, replicas are produced of the complementary faces generated above and below a single cleavage plane. All such experiments on chloroplasts (67), red cell membranes (70), and nexus membranes (Bullivant, personal communication; 64) show that a single cleavage plane generates both faces A and B of these membranes. Consideration of the thickness of the two lamellae that comprise nonjunctional membranes indicates that the unique cleavage plane exists near the anatomic center of such membranes (5, 70). However, the cleavage of nexus membranes may be asymmetric (see below). In surface labeling experiments, distinctive markers are added to the membrane's outer surface. Examination of labeled red cells has shown that the markers are not seen on the cleaved faces but are only on the surfaces which are revealed after etching in distilled water (56, 57, 66). These experiments demonstrate that the faces revealed by cleaving are not at the surface of the membrane. Taken together, double replica and labeling experiments strongly support the membrane-splitting hypothesis of Branton (5), who originally recognized that the two membrane faces revealed by cleaving are located within the membrane's interior and are usually produced by the cleavage plane splitting the membrane into two lamellae.

Data obtained from replicas of nexuses in near cross-fracture can be explained on the basis of membrane-splitting, although a slightly eccentric cleavage within each membrane is needed to account for the observed measurements of thick-

[5] The actual values for junction thickness depend on how the measurements are made. Important variables include tissue fixation, section thickness, intensity of staining, accuracy of microscope calibration, and whether the measurements are of total stained thickness or distance from peak to peak on a microdensitometer trace. In our laboratory, the total thickness of stainable membrane material at the zonula occludens is usually approximately 140 A, compared to 170–190 A for the nexus, when the nonjunctional plasma membrane measures 75 A. Some investigators have reported slightly different dimensions, such as 135–150 A for the nexus (7, 25, 62) in central nervous system and liver. However, the stated relationship of the thickness of the junctions relative to the thickness of nonjunctional "unit" plasma membrane in the same preparations has been confirmed (7).

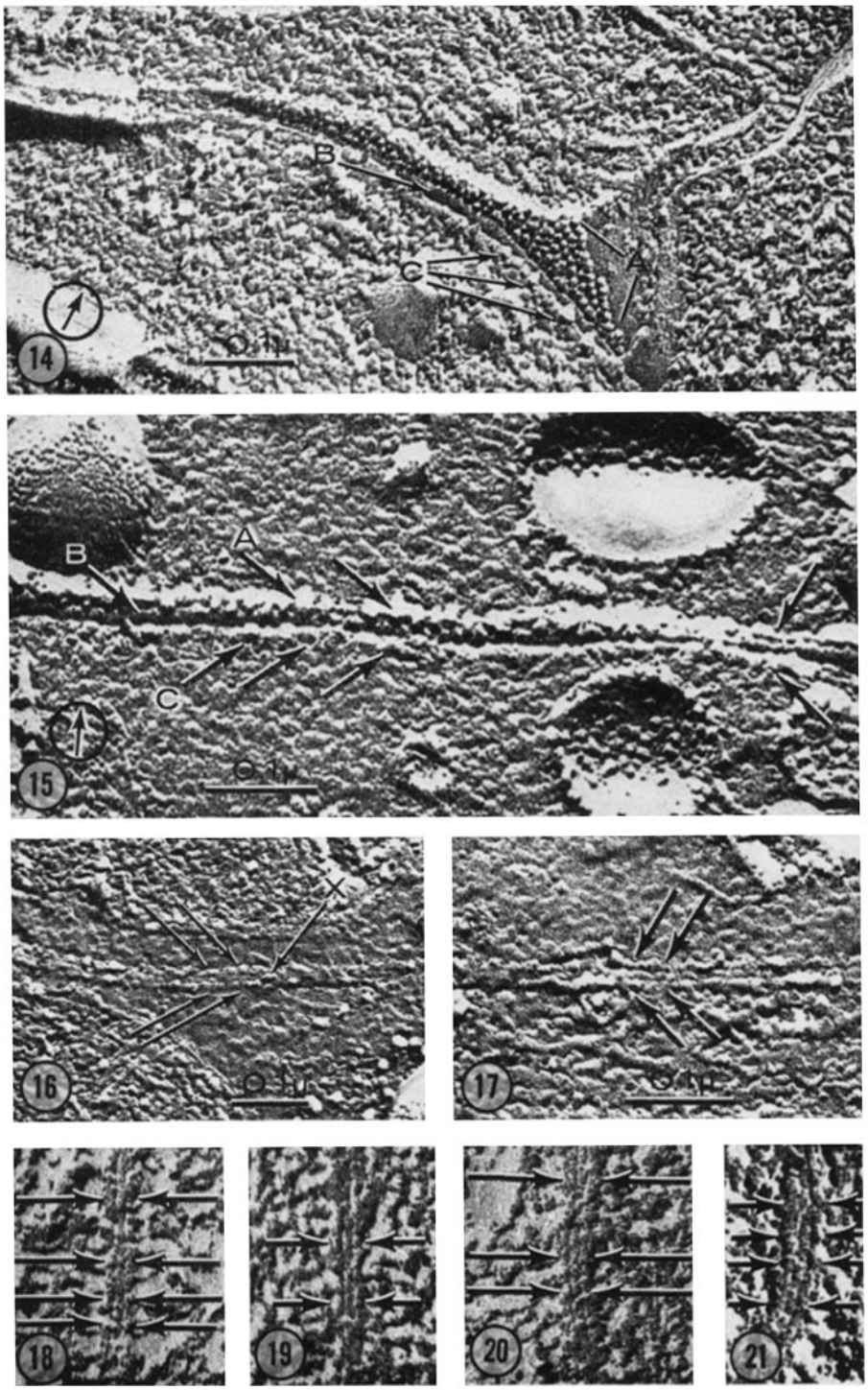
B
A
C
14
0.1 μ
B
A
C
15
0.1 μ
X
16
0.1 μ
17
0.1 μ
18
19
20
21

ness of the lamellae. At the nexus, the cleaving of two membranes into three equal ridges would be accomplished if the cleavage plane deviated from its usual central or 1:1 position in the nonjunctional membrane to an approximately 2:1 position within each nexus membrane. Such a change in the level of the cleavage may explain the narrow, smooth rim of membrane face adjacent to the nexus faces A and B. An apparent change in the level of the cleavage plane could also be explained by a localized increase in the thickness of the inner membrane lamella (Lm 1) at the nexus (Fig. 9).

Although we accept the hypothesis that face A and face B represent two faces generated by cleaving the interior of the plasma membrane, the observation that the fine features of the two faces are not exactly complementary deserves comment. At the nexus, face A and face B are very close to being complementary, except for the apparent sizes of the particles on face A and the pits on face B. The nonjunctional membrane face A and face B are much further from being complementary, since few pits are visualized in either face. Some distortion from complementarity of the faces could be produced by plastic deformation of structures during cleaving (12), although such deformation has not been shown for membranes. The shadowing and replicating procedures are known to introduce distortions of detail; some of the size distortion has been evaluated, and correction factors for these distortions have been calculated (27, 38, 45). When a fracture face is shadowed at an angle, electron-opaque shadowing material accumulates on projecting structures, enlarging their apparent dimensions and shifting their apparent central axis towards the shadowing source. Depressions or pits in the surfaces tend to be filled with shadowing material, and may have their apparent centers slightly shifted toward the shadowing source. Depressions are reduced in apparent diameter, and, with heavy shadowing, may be obliterated. Other possible sources of distortion include water vapor, hydrocarbons, and other contaminants within the vacuum system which may be adsorbed onto the cold fracture face (36). If contaminants were to condense on the fracture face prior to replication, the fracture face may have enlarged projections, obscured pits, and otherwise decorated faces. Although the relative contributions of these various factors have yet to be systematically analyzed, the presence of the central tier in the Bullivant Type II device appears to provide effective cryotrapping of contaminants, and minimizes these distortions (Weinstein and McNutt, data in preparation).

Relation of Face A Particulate Component to the Lanthanum-Outlined Subunits of Thin Sections

The subunits outlined by lanthanum in thin sections, the particles on nexus face A, and the pits on nexus face B, each show 90–100 A center-to-center spacing in the most highly ordered areas. If, prior to fracture, the pits on face B were

---

Two illustrations of nexuses in oblique fracture, and six examples of nexuses in cross-fracture in etched preparations. Encircled arrow indicates the direction of platinum shawdowing.

FIGURE 14 In this nexus in oblique fracture, the three layers of the nexus are visible with small portions of faces *A*, *B*, and *C* exposed. The particles of nexus face A are closely packed. The edge of nexus face C appears coarsely granular, suggesting a layer of closely packed globular components. × 124,000.

FIGURE 15 This nexus is seen in a less oblique fracture than Fig. 14. At the left, the edges of each of the three layers can be found, each having a rather granular appearance. At the right, the nexus is seen at even less oblique fracture and is still composed of three layers. × 154,000.

FIGURES 16–21 In these six examples, very nearly cross-fractured nexuses are illustrated. In each case, the nexus is composed of three layers, each of which has a rather granular appearance, but the particles do not seem to extend beyond their own layer. In Fig. 16, a distinct central particle is evident (*X*). The adjacent cytoplasm appears rather granular in these etched preparations. The direction of shadowing is from the bottom of the print in Figs. 16–18, and 20. The shadowing direction is from the right on Fig. 19 and from the left on Fig. 21. In each picture the double and multiple sets of arrows indicate the boundaries of the nexus. Fig. 16, × 105,000, Fig. 17, × 150,000, Figs. 18–21, × 150,000.

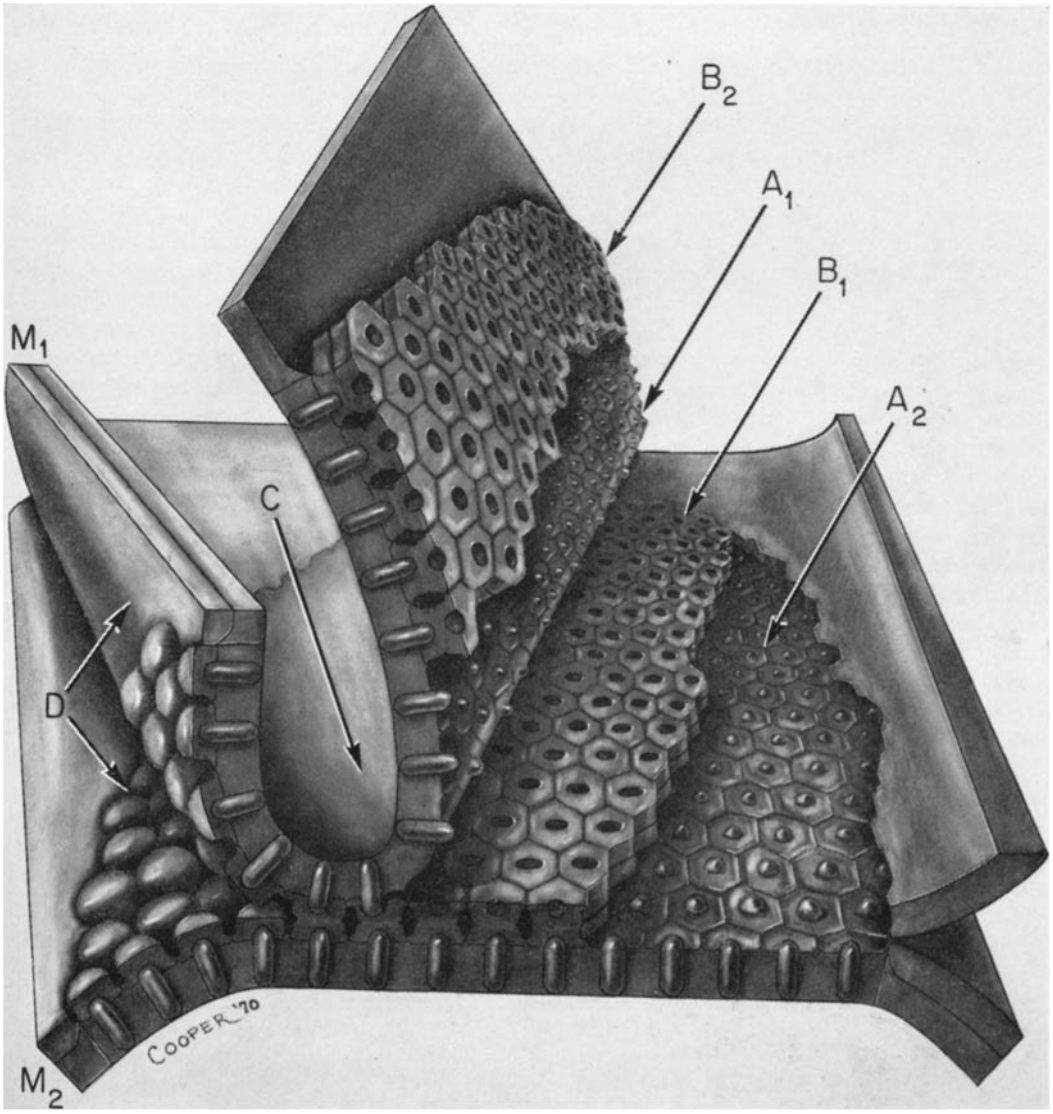

FIGURE 22 Artist's drawing of the interrelation of the nexus faces exposed by cleaving and the subunits seen in thin-sectioned and freeze-cleaved nexuses. On the left, the manner of contact of the two plasma membranes (M_1 and M_2) is illustrated. The appearance of the Face D of each of these membranes is deduced from thin sections since this aspect of the membranes is not revealed by cleaving ordinary preparations. On the right, the cleavage plane has split open a nexus by first cleaving into the interior of membrane 2 and then passing into the interior of membrane 1. Each membrane is cleaved into two lamellae, one of which has a face A and the other of which has a face B. If the upper portion of the specimen is retrieved as well as the bottom portion of the specimen, it has been shown that matching areas of face A and face B are found (Bullivant, personal communication). Also, the drawing indicates how the nexus face B is always seen on a layer which is on top of a nexus face A, if both are visualized in the same nexus. The nexus face C represents the true juxtacytoplasmic surface of the nexus. No ordered structure has been revealed for this face. The edge of this juxtacytoplasmic layer has a rather granular appearance, indicating that the particles visualized on nexus face A may extend through the full thickness of the layer.

apposed to the intersection of particles on face A, then a different center-to-center spacing would be expected for the pits compared to the particles. Since the particles on face A and the pits on face B both show approximately 90 A spacing, it is likely that the particles on one face and the pits on the other are in register (i.e. the particles on face A fit into or over the pits on face B). Also, the pits and the particles demonstrated by freeze-cleaving probably exist in register with the subunits outlined by lanthanum in thin sections.

When the face A particles were first observed, it was thought that they represented the subunits seen in thin-sectioned material (37, 43). However, acceptance of the membrane-splitting hypothesis requires modification of this earlier interpretation (Fig. 22). It now appears that the subunits demonstrated with lanthanum in thin sections are in the central 60 A zone of the junction, whereas the face A particles of freeze-cleave preparations are components of the two juxtacytoplasmic lamellae of the freeze-cleaved nexus membrane complex. Since the face A particles project from the surface of the lamella 1, these face A particles could fit into the pits of face B of lamella 2. The subunits of lamella 2 presumably represent caps over the ends of the face A particles. These subunits would in turn project from the face D of lamella 2 and contact their counterparts from the apposed membrane at the central plane of the nexus. It would be the face D aspects of the subunits of lamella 2 of each membrane which correspond to the subunits outlined by lanthanum as seen in thin sections. The appearance of face D is deduced from the thin-section appearance, since this face is not revealed by either freeze-cleaving or heat-etching.

The suggestion that face A particles protrude into the pits of face B subunits is consistent with data on the size of the particles and the subunits. For this arrangement, we would expect the face A particles to be somewhat smaller than the protruding cap of the subunits at face D. The diameter of the face D cap is estimated from the measurements of the subunits outlined by lanthanum in thin sections. Presumably, the lanthanum fills thin channels coursing around small columns formed by the fusion of the projecting caps of face D subunits. According to such measurements, the caps are approximately 70 A in diameter. This is consistent with data obtained by negative staining (3, 25). As measured in replicas, the particles on face A measure from 55 to 75 A in diameter. However, their estimated actual size is smaller, since a correction factor for the size increase introduced by the replicating procedure must be employed. An exact correction factor cannot be used, since the angle of shadowing for a given area of a curved membrane cannot be calculated. However, according to the method of Misra and Das Gupta (45) as applied by Lessin et al. (38), an estimate that the actual dimensions are approximately 2/3 of the measured dimensions seems reasonable. The face A particles would then measure from 40 to 50 A in actual diameter, and would be substantially smaller than the subunit caps at face D.

From a biochemical standpoint, a face A particle and a face B subunit, into which it inserts, may be portions of a macromolecular assembly that is cleaved at low temperatures into face A and B components. The preferential binding of face A particles to Lm 1 rather than to the face B subunits during cleaving might eventually give important clues as to the nature of the chemical bonds within the macromolecular assembly.

The structures visualized by freeze-cleaving which suggest a central channel in the nexus subunits are (*a*) the pits visualized in the central stratum subunits at face B, and (*b*) the central depressions in the particles seen on face A of the juxtacytoplasmic lamella (Lm 1). The features suggesting a central channel in thin sections are (*a*) the central dot observed by Robertson at electrical synapses (62), and (*b*) the central dot revealed by lanthanum tracer (60).

Physiologic Correlates of Ultrastructural Data

Physiologic evidence indicates that a hydrophilic channel connects the interiors of the cells apposed at the nexus without connecting either interior to the extracellular space (4, 23, 39, 55). We would speculate that a hydrophilic channel may pass through the center of the nexus subunits as in Fig. 23. The minimal dimensions of such trans-nexus channels can be approximated from the size of molecular probes that pass from cell to cell through the nexus. The observation that the dye Procion yellow M4RS (mol wt approximately 500) (I. C. I. America Inc., Stamford, Conn.) and sucrose (mol wt 342) pass from cell to cell through the nexus (4, 55) indicates that some of the trans-nexus channels are in the range of 15–20 A in diameter. Molecular probes necessary to determine

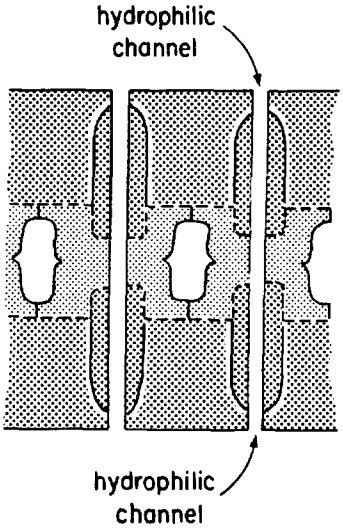

FIGURE 23 An interpretation of the position of the hydrophilic channel in the nexus subunits. Segments of such a channel have been demonstrated. A hydrophilic channel is necessary to account for the cell-to-cell transport of small ions (see text). This diagram is not drawn to an exact scale.

a maximum size have not been employed. Quantitation of specific nexus resistance, by electrophysiologic measurements, should allow an estimate of the transnexus channel size which would produce the observed potassium permeability of the nexus (35, 68, 71). However, at present many assumptions are necessary for such a calculation, and the result may easily be inadequate because the area of cell surface covered by nexus is difficult to estimate (35, 68, 72). We would speculate that at least portions of the hypothetical transnexus channels may be visible in the replicas as the central pits in the nexus face A particles and face B subunits. Taking into account the shadowing distortion, these channels at the level visualized are probably in the range of 30–40 A in diameter in the region exposed by cleavage. Since the channels have not been seen in their full extent, it is premature to speculate that the diameter of such a channel is uniform throughout. If the channel orifice in nexus face C is on the order of 20 A in diameter, then this aspect of the channel would be below the present limit of resolution of the freeze-cleave technique (47).

The particulate component on face A of lamella 1 and the subunits of lamella 2 have not been isolated and chemically characterized. Goodenough and Revel (25) have reported the extraction of nexuses of liver with 60% acetone and have shown in thin sections that the staining appearance of a central lucent zone or "gap" at the nexus is dependent on the presence of lipid at the time of osmium tetroxide fixation of the junction. They also reported that the disappearance of the "gap" is simultaneous with the disappearance of evidence of face A particles in acetone-extracted, freeze-cleaved material, implying that the particles reside in the "gap." However, their failure to visualize face A particles may be spurious because lipid-extracted membranes can retain their thin-section appearance (21, 52), but they may not deviate a cleavage plane (5), thereby eliminating the *en face* view of the surfaces bearing the particles. Under conditions of partial lipid extraction, the presence of cleavage planes in some areas of the membranes does not rule out the loss of cleavage planes in other areas. Elucidation of the chemical nature of the nexus subunits still awaits their isolation in pure form.

The evidence to date favors the interpretation that the nexus contains a closely packed array of subunits within the interior of each of the membranes. The size of the subunits and the presence of a potential cleavage plane within each membrane are most compatible with the hypothesis that the subunits observed all represent different aspects of a complex macromolecular assembly. In order for the nexus to provide efficient electrical coupling of cells, it must provide channels which are nonleaky and which bridge the major permeability barriers to potassium at the adjacent cell surfaces. A central hydrophilic channel passing through the subunit assembly could provide this function.

The authors gratefully acknowledge the advice of Professor Don W. Fawcett in useful discussions of this work and in critically reviewing the manuscript. We thank Professor Herbert Fischer of the Max Planck Institut für Immunbiologie in Freiburg, Germany, and Professor Peter Sitte of the University of Freiburg, for the use of their Balzers Freeze-Etch device, and Mr. Volker Speth for technical assistance in preparing replicas with method II. The technical assistance of Mr. Frederick B. Merk, Miss Joyce Jakobsen, and Miss Songza Ahn is appreciated, as is the assistance of Miss Linda Kaufman in preparing the manuscript, and Mr. David Lang and Miss Gail Cooper in preparing the illustrations.

This study was supported by National Cancer Institute Grant CA-07368 from the National In-

stitutes of Health, and United States Public Health Service Training Grant T01-GM00192. Part of this work was completed by Dr. McNutt as a post-doctoral fellow at the Department of Anatomy, Harvard Medical School, with support from Research Grants GM-06729 and GM-406TG from the Institute of General Medical Sciences, United States Public Health Service.

Received for publication 20 April 1970, and in revised form 23 June 1970.

REFERENCES

1. BARR, L., W. BERGER, and M. M. DEWEY. 1968. *J. Gen. Physiol.* **51**:347.
2. BARR, L., M. M. DEWEY, and W. BERGER. 1965. *J. Gen. Physiol.* **48**:797.
3. BENEDETTI, E. L., and P. EMMELOT. 1968. *J. Cell Biol.* **38**:15.
4. BENNETT, M. V. L., and P. B. DUNHAM. 1970. Abstracts of the Biophysical Society, 14th Annual Meeting, Biophysical Society, New York. 114 a.
5. BRANTON, D. 1966. *Proc. Nat. Acad. Sci. U. S. A.* **55**:1048.
6. BRANTON, D. 1969. *Annu. Rev. Plant Physiol.* **20**: 209.
7. BRIGHTMAN, M. W., and T. S. REESE. 1969. *J. Cell Biol.* **40**:648.
8. BULLIVANT, S. 1969. *Micron.* **1**:46.
9. BULLIVANT, S., and A. AMES, III. 1966. *J. Cell Biol.* **29**:435.
10. BULLIVANT, S., and R. S. WEINSTEIN. 1969. *Anat. Rec.* **163**:296.
11. BULLIVANT, S., R. S. WEINSTEIN, and K. Someda. 1968. *J. Cell Biol.* **39** (2, Pt. 2):19 a (Abstr.).
12. CLARK, A. W., and D. BRANTON. 1968. *Z. Zell. forsch. Mikrosk. Anat.* **91**:586.
13. DEWEY, M. M., and L. BARR. 1962. *Science (Washington).* **137**:670.
14. DEWEY, M. M., and L. BARR. 1964. *J. Cell Biol.* **23**:553.
15. DREIFUSS, J. J., L. GIRARDIER, and W. G. FORSSMANN. 1966. *Pflugers Arch. Gesamte Physiol. Menschen Tiere.* **292**:13.
16. FARQUHAR, M. G., and G. E. PALADE. 1963. *J. Cell Biol.* **17**:375.
17. FARQUHAR, M. G., and G. E. PALADE. 1964. *Proc. Nat. Acad. Sci. U. S. A.* **51**:569.
18. FARQUHAR, M. G., and G. E. PALADE. 1965. *J. Cell Biol.* **26**:263.
19. FAWCETT, D. W. 1966. *In* The Cell: its organelles and inclusions. W. B. Saunders Company, Philadelphia, Pa. 374.
20. FAWCETT, D. W., and N. S. MCNUTT. 1969. *J. Cell Biol.* **42**:1.
21. FLEISCHER, S., B. FLEISCHER, and W. STOECKENIUS. 1967. *J. Cell Biol.* **32**:193.
22. FRIEDERICI, H. H. R. 1969. *Lab. Invest.* **21**:459.
23. FURSHPAN, E. J., and D. D. POTTER. 1968. *In* Current Topics in Developmental Biology. A. Moscona and A. Monroy, editors. Academic Press Inc., New York. **3**:95.
24. GLASER, M., H. SIMPKINS, S. J. SINGER, M. SHEETZ, and S, I. CHAN. 1970. *Proc. Nat. Acad. Sci. U. S. A.* **65**:721.
25. GOODENOUGH, D. A., and J. P. REVEL. 1970. *J. Cell Biol.* **45**:272.
26. HACKEMANN, M., C. GRUBB, and K. R. HILL. 1968. *J. Uultrstruct. Res.* **22**:443.
27. HALL, C. E. 1960. *J. Biophys. Biochem. Cytol.* **7**: 613.
28. KARNOVSKY, M. J. 1965. *J. Cell Biol.* **27**:137 A. (Abstr.)
29. KARRER, H. E. 1960. *J. Biophys. Biochem. Cytol.* **7**:181.
30. KARRER, H. E. 1960. *J. Biophys. Biochem. Cytol.* **8**:135.
31. KAWAMURA, K., and T. KONISHI. 1967. *Jap. Circ. J.* **31**:1533.
32. KELLENBERGER, E., A. RYTER, and J. SECHAUD. 1958. *J. Biophys. Biochem. Cytol.* **4**:671.
33. KOEHLER, J. K., 1968. *Advan. Biol. Med. Phys.* **12**:1.
34. KORN, E. D. 1966. *Science (Washington).* **153**:1491.
35. KREIBEL, M. E. 1968. *J. Gen. Physiol.* **52**:46.
36. KREUTZIGER, G. O. 1968. *In* Proceedings of the 26th Meeting of the Electron Microscopy Society of America. Claitor's Publishing Division, Baton Rouge, La. 138.
37. KREUTZIGER, G. O. 1968. *In* Proceedings of the 26th Meeting of the Electron Microscopy Society of America. Claitor's Publishing Division, Baton Rouge, La. 234.
38. LESSIN, L. S., W. N. JENSEN, and E. PONDER. 1969. *J. Exp. Med.* **130**:443.
39. LOEWENSTEIN, W. R. 1966. *Ann. N. Y. Acad. Sci.* **137**:441.
40. LUFT, J. H. 1961. *J. Biophys. Biochem. Cytol.* **9**:409.
41. MATTER, A., L. ORCI, and C. ROUILLER. 1969. *J. Ultrastruct. Res. Suppl.*, **11**:5.
42. MCNUTT, N. S. 1970. *Amer. J. Cardiol.* **25**:169.
43. MCNUTT, N. S., and R. S. WEINSTEIN. 1969. *In* Proceedings of the 27th Meeting of the Electron Microscopy Society America., Claitor's Publishing Division, Baton Rouge, La. 330.
44. MCNUTT, N. S., and R. S. WEINSTEIN. 1970. Abstracts of the Biophysical Society, 14th Annual Meeting Biophysical Society New York. 101 a.
45. MISRA, D. N., and N. N. DAS GUPTA. 1966. *J. Roy. Microsc. Soc.* **84**:373.
46. MOOR, H. 1959. *J. Ultrastruct. Res.* **2**:393.

47. MOOR, H. 1966. *Int. Rev. Exp. Pathol.* **5**:179.
48. MOOR, H., K. MÜHLETHALER, H. WALDNER, and A. FREY-WYSSLING. 1961. *J. Biophys. Biochem. Cytol.* **10**:1.
49. MÜHLETHALER, K., H. MOOR, J. W. SZARKOWSKY. 1965. *Planta.* **67**:305.
50. MUIR, A. R. 1965. *J. Anat.* **99**:27.
51. MUIR, A. R. 1967. *J. Anat.* **101**:239.
52. NAPOLITANO, L., F. LEBARON, and J. SCALETTI. 1967. *J. Cell Biol.* **34**:187.
53. PARK, R. B., and A. O. PFEIFHOFER. 1969. *J. Cell Sci.* **5**:299.
54. PARK, R. B., and A. O. PFEIFHOFER. 1969. *J. Cell Sci.* **5**:313.
55. PAYTON, B. W., M. V. L. BENNETT, and G. D. PAPPAS. 1969. *Science (Washington).* **166**:1641.
56. PINTO DA SILVA, P., and D. BRANTON. 1969. 11th International Botanical Congress Abstracts. Botanical Society, Seattle, Wash. 171.
57. PINTO DA SILVA, P., and D. BRANTON. 1970. *J. Cell Biol.* **45**:598.
58. RAYNS, D. G., F. O. SIMPSON, and W. S. BERTAUD. 1968. *J. Cell Sci.* **3**:467.
59. REVEL, J. P. 1968. *In* Proceedings of the 26th Meeting of the Electron Microscopy Society of America, Claitor's Publishing Division, Baton Rouge, La. 40.
60. REVEL, J. P., and M. J. KARNOVSKY. 1967. *J. Cell Biol.* **33**:C7.
61. ROBERTSON, J. D. 1959. *Biochem. Soc. Symp.* **16**:3.
62. ROBERTSON, J. D. 1963. *J. Cell Biol.* **19**:201.
63. SJÖSTRAND, F. S., E. ANDERSSON-CEDERGREN, and M. M. DEWEY. 1958. *J. Ultrastruct. Res.* **1**: 271.
64. SOMMER, J. R., and E. A. JOHNSON. 1970. *Amer. J. Cardiol.* **25**:184.
65. STAEHELIN, L. A. 1968. *J. Ultrastruct. Res.* **22**: 326.
66. TILLACK, T. W., and V. T. MARCHESI. 1970. *J. Cell Biol.* **45**:649.
67. WEHRLI, E., K. MÜHLETHALER, and H. MOOR. 1970. *Exp. Cell Res.* **59**:336.
68. WEIDMANN, S. 1966. *J. Physiol. (London).* **187**:323.
69. WEINSTEIN, R. S. 1969. *In* Red Cell Membrane Structure and Function. G. A. Jamieson and T. J. Greenwalt, editors. J. B. Lippincott Co., Philadelphia, Pa. 36.
70. WEINSTEIN, R. S., A. CLOWES, and N. S. MCNUTT. 1970 *Proc. Soc. Exp. Biol. Med.* **134**:1195.
71. WEINSTEIN, R. S., and N. S. MCNUTT. 1970. Seminars in Hematology. **7**:259.
72. WOODBURY, J. W., and W. E. CRILL. 1961. *In* Nervous Inhibition. E. Florey, editor. Pergamon Press Inc., New York. 124.